

# Role of $\text{Mg}^{2+}$ Ions in the Conformational Change Reported by Fluorescein 5'-Isothiocyanate Modification of $\text{Na}^+, \text{K}^+$ -ATPase<sup>†</sup>

Irina N. Smirnova and Larry D. Faller\*

Center for Ulcer Research and Education, Department of Medicine, University of California at Los Angeles School of Medicine, and Wadsworth Division, Department of Veterans Affairs, Medical Center West Los Angeles, Los Angeles, California 90073

Received November 24, 1992; Revised Manuscript Received March 4, 1993

**ABSTRACT:** The role of  $\text{Mg}^{2+}$  in the conformational change reported by fluorescein 5'-isothiocyanate modification of  $\text{Na}, \text{K}$ -ATPase has been studied by stopped-flow fluorometry.  $\text{K}^+$  causes a fluorescence quench that is reversed by  $\text{Na}^+$ . The principal experimental observations are as follows: (1)  $\text{Mg}^{2+}$  decreases the apparent affinity of the enzyme for  $\text{K}^+$  but does not affect the maximum rate of the  $\text{K}^+$  quench. (2) The amplitude of the  $\text{K}^+$  quench depends hyperbolically on the  $\text{K}^+$  concentration, and the maximum amplitude is unaffected by the  $\text{Mg}^{2+}$  concentration. (3) The rate at which  $\text{Na}^+$  reverses the  $\text{K}^+$  quench depends inversely on the  $\text{Mg}^{2+}$  concentration. (4) The amplitude of the  $\text{Na}^+$  reversal also decreases with increasing  $\text{Mg}^{2+}$  concentration. The data are quantitatively explained by a model that assumes only two enzyme conformations, detectable by their fluorescence emission.  $\text{Mg}^{2+}$  increases  $K_d$  for  $\text{K}^+$  from 14 to 223 mM. At 22 °C,  $K_d = 0.16$  mM for  $\text{Mg}^{2+}$  dissociation from  $\text{E}_1$ , and the heat of  $\text{Mg}^{2+}$  binding,  $\Delta H^\circ$ , is 11.4 kcal  $\text{mol}^{-1}$ .  $K_d$  is more than an order of magnitude larger for  $\text{Mg}^{2+}$  dissociation from  $\text{E}_2\text{K}$ .  $\text{Mg}^{2+}$  binding does not affect the forward ( $\text{E}_1\text{K} \rightarrow \text{E}_2\text{K}$ ) rate constant ( $k_f$ ), but decreases the reverse rate constant ( $k_r$ ) thus increasing the equilibrium constant for the reaction ( $K_c = k_f/k_r$ ) 6-fold. Therefore,  $\text{Mg}^{2+}$  is not directly involved in the conformational transition, but the study supports proposals that  $\text{Mg}^{2+}$  binding and release may help to regulate the transport cycle by shifting the distribution of enzyme between  $\text{E}_1$  and  $\text{E}_2$  conformers.

The central hypothesis in models for active transport by P-type ion-motive ATPases is that the enzyme exists in two conformations designated  $\text{E}_1$  and  $\text{E}_2$ . Energy coupling is explained by different chemical reactivity of the two conformations, and ion transport is explained by opposite orientation of the ion binding sites with respect to the plane of the membrane in the two conformations. What are not known are the molecular details of the conformational change. The specific question asked in this paper is whether the conformational transition depends upon the divalent cation that is required for activity.

Karlish (1980) showed that the conformational change in the dephosphoenzyme is reported by FITC<sup>1</sup> labeling of the enzyme and proposed a mechanism to explain how the transported ions  $\text{Na}^+$  and  $\text{K}^+$  cause the transition. We have shown that the mechanism of the conformational step can be studied by measuring the forward and reverse rates and amplitudes of the transition as a function of temperature (Faller et al., 1991b). We are systematically exploiting this approach by investigating the individual chemical components of the pump to learn which of them are involved in the transition state between  $\text{E}_1$  and  $\text{E}_2$  and to elucidate the role of those that are reactants in the conformational change.

In an initial study, we compared the  $\text{E}_1\text{K} \rightleftharpoons \text{E}_2\text{K}$  transition in  $\text{Na}, \text{K}$ -ATPase reported by fluorescein with the corresponding conformational change in  $\text{H}, \text{K}$ -ATPase (Faller et al., 1991a). In both enzymes the barrier to reaction is an increase in enthalpy that is partially compensated by increased entropy in the transition state. The change in  $\text{Na}, \text{K}$ -ATPase from the  $\text{E}_1\text{K}$  conformation to the  $\text{E}_2\text{K}$  conformation is exothermic, and the entropy of the final state is lower than the entropy of the initial state, consistent with "occlusion" of the transported ion (Post et al., 1972). The reaction is exergonic, equilibrium favoring the  $\text{E}_2\text{K}$  conformer by almost 3 orders of magnitude. In sharp contrast, the conformational change in  $\text{H}, \text{K}$ -ATPase reported by fluorescein is approximately isoenergetic. The fundamental difference between the two enzymes is that the  $\text{E}_2\text{K} \rightarrow \text{E}_1\text{K}$  transition of  $\text{H}, \text{K}$ -ATPase is more than 2 orders of magnitude faster than the corresponding reaction of  $\text{Na}, \text{K}$ -ATPase (Faller et al., 1990), explaining failure to observe a  $\text{K}^+$ -occluded form of  $\text{H}, \text{K}$ -ATPase (De Pont et al., 1985). Unless chemical modification with fluorescein is causing the difference in rate of the  $\text{E}_2\text{K} \rightarrow \text{E}_1\text{K}$  transition between  $\text{H}, \text{K}$ -ATPase and  $\text{Na}, \text{K}$ -ATPase, rate limitation does not appear to occur at the same step in the reaction cycles of the two enzymes, and it is unnecessary to postulate low-affinity nucleotide acceleration of the  $\text{E}_2\text{K} \rightarrow \text{E}_1\text{K}$  conformational change in  $\text{H}, \text{K}$ -ATPase to explain *in vitro* and *in vivo* turnover numbers, or the rate of active ion fluxes. Therefore, an intermediate in which the transported ion is occluded may not be a general feature of P-type ion-motive ATPases.

In this paper we report stopped-flow experiments designed to investigate the effect of the divalent cation required for physiological function on both the forward and the reverse rate of the  $\text{E}_1\text{K} \rightleftharpoons \text{E}_2\text{K}$  conformational change in  $\text{Na}, \text{K}$ -ATPase. Glynn (1985) has reviewed published studies of how  $\text{Mg}^{2+}$  affects the conformational change. The principal conclusions drawn from experiments with FITC-labeled

<sup>†</sup> This work was supported by a Veterans Administration Merit Review Award and by U.S. Public Health Service Grant DK36873 and National Science Foundation Grant MCB9106338 awarded to L.D.F.

<sup>1</sup> Abbreviations:  $\text{Na}, \text{K}$ -ATPase,  $\text{Mg}^{2+}$ -dependent,  $\text{Na}^+$ - and  $\text{K}^+$ -stimulated ATPase (EC 3.6.1.37);  $\text{H}, \text{K}$ -ATPase,  $\text{Mg}^{2+}$ -dependent,  $\text{H}^+$ -transporting,  $\text{K}^+$ -stimulated ATPase (EC 3.6.1.36); enolase, 2-phospho-D-glycerate hydrolyase (EC 4.2.1.11); ATP, adenosine 5'-triphosphate; CoATP,  $\beta, \gamma$ -bidentate complex of  $\text{Co}^{3+}$ ,  $\text{NH}_3$ , and ATP; CrATP,  $\beta, \gamma$ -bidentate complex of  $\text{Cr}^{3+}$  and ATP; pNPP, *p*-nitrophenyl phosphate; FITC, fluorescein 5'-isothiocyanate; SDS, sodium dodecyl sulfate; EDTA, ethylenediaminetetraacetic acid; ChoCl, choline chloride; Tris, tris-(hydroxymethyl)aminomethane; DMSO, dimethyl sulfoxide;  $\text{P}_i$ , inorganic phosphate; EPR, electron paramagnetic resonance; NMR, nuclear magnetic resonance; SD, standard deviation.

enzyme are as follows: first,  $Mg^{2+}$  increases the intensity of fluorescence emitted by the  $E_2K$  conformer (Karlish, 1980); second,  $Mg^{2+}$  changes the shape of titration curves (fluorescence intensity versus  $[K^+]$ ) from hyperbolic to sigmoidal; and third, the rate of the  $E_2K \rightarrow E_1K$  reaction is inversely related to  $Mg^{2+}$  concentration (Hegyvary & Jorgensen, 1981). The consensus explanation of these observations is that  $Mg^{2+}$  induces a new conformation of the enzyme distinguishable by its fluorescence level. Our results confirm that  $Mg^{2+}$  binding decreases the rate of the  $E_2K \rightarrow E_1K$  transition but do not support the conclusion that there is a different conformation of the metalloenzyme.<sup>2</sup> We show that the effects of  $Mg^{2+}$  can be explained by a model in which the affinity of Na,K-ATPase for transported ions and the rate of the  $E_2K \rightarrow E_1K$  conformational change are different in the apo- and metalloenzymes, but the quantum yield of fluorescein in the  $E_1$  and  $E_2$  conformations is unaffected by divalent cation. We conclude that  $Mg^{2+}$  is not a reactant in the conformational transition, but our study supports speculation that  $Mg^{2+}$  binding and release may play an important role in regulating transport (Hegyvary & Jorgensen, 1981).

## EXPERIMENTAL PROCEDURES

### Materials

**Na,K-ATPase.** Membrane fragments containing Na,K-ATPase were isolated from the outer medulla of hog kidneys. The enzyme was purified by extracting nonintegral membrane proteins with SDS (Jorgensen, 1974). The preparations used in the reported experiments had specific Na,K-ATPase activities in the range 12–16  $\mu\text{mol min}^{-1}$  per mg of protein at 37 °C.

**Chemical Modification.** The enzyme was reacted with FITC at pH 9.2 using the experimental protocol published previously (Carilli et al., 1982). The measured relaxation times were independent of labeled-enzyme preparation, but the maximum percentage change in fluorescence varied from 9.3 to 15.5%. The chemically modified enzyme could be recycled and used in multiple experiments, as previously described (Faller et al., 1991a).

**Reagents.** Fluorescein 5'-isothiocyanate (isomer 1) was purchased from Molecular Probes. The chlorides of choline, magnesium, potassium, and sodium were obtained from Sigma. All other reagents were the highest grade commercially available.

### Methods

**Stopped-Flow Measurements.** The stopped-flow instrument described previously (Faller et al., 1991a) was modified by installing a T-mixer, which has an improved dead time ( $t_d$ ) equal to  $2.2 \pm 0.7$  ms, for mixing 200  $\mu\text{L}$  of solution at a 7-bar drive pressure and 23 °C. In addition to limiting the rate of reactions that can be measured,  $t_d$  is important for correction of observed amplitudes ( $\Delta F$ ) when the rate is so fast that only a fraction of the reaction can be seen (Faller et al., 1991a; eq 2). Corrected amplitudes ( $\Delta F_0$ ) are reported as percentage changes in fluorescence, i.e., fractions of the offset ( $F$ ), or final signal level in an experiment, expressed as percentages. This means that there is a systematic difference between the

maximum percentage change expected in quench and reversal experiments (see below), because the reference in the former experiments is the emission level of  $E_2$ , and in the latter it is the fluorescence of  $E_1$ .

In stopped-flow experiments, the objective is to keep all the variables constant before and after mixing except the reactant concentration that is perturbed. For example, ChoCl was used to avoid a simultaneous ionic strength jump. Unfortunately, enzyme dilution cannot be avoided, and in a few experiments where we wanted to titrate with >100 mM monovalent cation, or >33 mM  $MgCl_2$ , a control experiment was necessary. The pH was adjusted to correct for the effect of temperature on the ionization of Tris.

**Quench Experiments.** The fluorescence of FITC-modified Na,K-ATPase is quenched by  $K^+$ . Unless otherwise indicated, in quench experiments 100  $\mu\text{L}$  of solution containing 160  $\mu\text{g mL}^{-1}$  of FITC-modified protein in 0.13 mM EDTA and buffered at pH 7.4 by 50 mM Tris-HCl, the desired concentration of  $MgCl_2$ , and enough ChoCl for an ionic strength ( $\mu$ ) due to added salt of 200 mM was mixed with an equal volume of the same buffer containing twice the desired final concentration of  $K^+$ , the same concentration of  $MgCl_2$ , and a lower concentration of ChoCl, so that mixing did not change  $\mu$ .

**Reversal Experiments.** The fluorescence quench is reversed by  $Na^+$ . In these experiments the enzyme syringe also contained 5 mM  $K^+$  compensated by lower ChoCl for the same  $\mu$ . The titrant syringe contained 5 mM  $K^+$ , the desired final concentration of  $MgCl_2$ , twice the desired final concentration of NaCl, and ChoCl adjusted to give  $\mu = 200$  mM from added salt.

**Equilibrium Fluorescence Measurements.** Conventional fluorescence measurements were made in a Perkin-Elmer LS 50 fluorometer at ambient temperature with stirring. It was necessary to mix larger volumes in equilibrium than in "kinetic" titrations and to use a lower concentration of enzyme to avoid saturation of the photomultiplier. Otherwise, exactly the same experimental conditions were used in stopped-flow and conventional fluorometric measurements.

**Analysis.** The stopped-flow experiments were analyzed as concentration-jump, relaxation experiments. This approach is valid even though the perturbation in a mixing experiment is large, because the conformational change reported by fluorescein is unimolecular. It has two advantages. First, referring to the estimated first-order time constant as a relaxation time ( $\tau$ ) emphasizes that it generally depends in a complex way on several equilibrium constants and several rate constants for individual steps in the reaction mechanism, and second, derivation of the relationship between the observed time constant and the rate and equilibrium constants for individual steps in different reaction models is simplified. Details of the derivations are discussed in the Appendix, where the relaxation expression and the amplitude expressions for the model we are proposing to explain the effect of  $Mg^{2+}$  on the rates of the  $K^+$  quench and the  $Na^+$  reversal are derived. Relaxation times and amplitudes were estimated by fitting the expression for a single exponential with offset to individual, 1000-point kinetic records with the successive integration routine (Matheson, 1987) in On-Line Instrument Systems' Kinfilt software. The rate constants and equilibrium constants in the model were estimated by fitting the derived analytical expressions to the estimates of  $1/\tau$  and amplitude with the curve-fit program in SigmaPlot 4.1 or with BMDP Statistical Software's derivative-free, nonlinear regression program.

<sup>2</sup> Attempts are sometimes made to distinguish quantitatively between metal-activated enzymes and metalloenzymes (Wold, 1971). By these criteria  $Mn^{2+}$  forms a metalloenzyme of Na,K-ATPase (Grisham & Mildvan, 1974), but Na,K-ATPase is  $Mg^{2+}$  activated. For convenience, we will refer to the enzyme with  $Mg^{2+}$  specifically bound as a metalloenzyme.

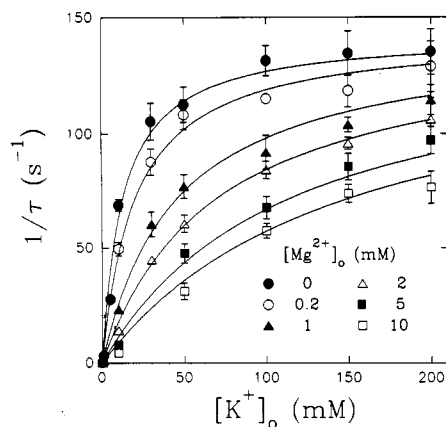


FIGURE 1: Effect of  $\text{Mg}^{2+}$  on  $1/\tau$  of  $\text{K}^+$  quench. Reciprocal relaxation time is plotted against  $[\text{K}^+]_0$  after mixing, as a function of  $[\text{Mg}^{2+}]_0$ . Each reactant solution contained the  $\text{MgCl}_2$  concentration shown and  $\text{ChoCl}$  in 50 mM Tris-HCL adjusted to pH = 7.4 at 15.0 °C. The  $\text{ChoCl}$  concentration was varied to keep the ionic strength of added monovalent and divalent cations constant at  $\mu = 200$  mM. The enzyme syringe also contained 160  $\mu\text{g mL}^{-1}$  protein and 0.13 mM Tris-EDTA. The ligand syringe contained twice the final concentration of KCl. Fluorescein was excited at 495 nm, and light emitted above 514 nm was detected as a proportional voltage. The drive pressure was 7 bar, and the electronic time constant was 0.1 ms. The mean  $1/\tau$  value estimated from 8–10 replicate measurements at each  $\text{K}^+$  and  $\text{Mg}^{2+}$  concentration is plotted. Vertical bars indicate the standard deviation, when SD exceeded the symbol size. The theoretical curves in the figure were calculated with the parameters in Table I that were estimated by fitting eq 2 to the entire array of  $\text{K}^+$ -quench data at 15 °C (details in text).

## RESULTS

The effect of  $\text{Mg}^{2+}$  concentration on the quench and reversal reactions has been studied as a function of temperature. Scatter plots of the 15 °C data are presented in Figures 1–4. Details of the experiments are given in the figure captions. The lines in the figures are theoretical curves calculated as described in the Discussion section.

**$1/\tau$  for  $\text{K}^+$  Quench.** Figure 1 is a scatter plot of  $1/\tau$  versus  $[\text{K}^+]_0$  at different  $\text{Mg}^{2+}$  concentrations. A tentative assessment of  $\text{Mg}^{2+}$ 's effects was obtained by fitting the equation derived previously to explain the dependence of  $1/\tau$  on  $[\text{K}^+]$  (Faller et al., 1991a; eq 4) to the data with  $k_{-2} = 0$ , because the reverse rate constant is too small compared to the measured  $1/\tau$  values for estimation. The estimates of the forward rate constant ( $k_2$ ) at different  $\text{Mg}^{2+}$  concentrations scatter about  $148 \pm 31 \text{ s}^{-1}$ . The estimates of  $K_K$ , the half-maximum  $\text{K}^+$  concentration, increase monotonically with  $[\text{Mg}^{2+}]$  from 14 mM (no  $\text{Mg}^{2+}$ ) to 169 mM (10 mM  $\text{Mg}^{2+}$ ). The corresponding estimates of  $k_2$  at 8 and 22 °C are  $60 \pm 9 \text{ s}^{-1}$  and  $335 \pm 10 \text{ s}^{-1}$ , respectively. The estimates of  $K_K$  increase with  $0 \leq [\text{Mg}^{2+}] \leq 10 \text{ mM}$  from 11 to 176 mM at 8 °C and from 15 to 163 mM at 22 °C. The results suggest that the rate constant for the  $\text{E}_1\text{K} \rightarrow \text{E}_2\text{K}$  transition is independent of  $[\text{Mg}^{2+}]$ , but the affinity of  $\text{E}_1$  for  $\text{K}^+$  appears to be inversely related to  $[\text{Mg}^{2+}]$ .

**Amplitude of  $\text{K}^+$  Quench.** The  $t_d$ -corrected amplitudes observed for the  $\text{K}^+$  quench in stopped-flow experiments at different  $\text{Mg}^{2+}$  concentrations are plotted against  $[\text{K}^+]_0$  in Figure 2a. A 1.6% correction was made to the data at 200 mM  $\text{K}^+$  for the simultaneous ionic strength jump that cannot be avoided at the highest titrant concentration. Fitting the equation for binding to a single class of sites to the data at each  $\text{Mg}^{2+}$  concentration separately gives estimates of the maximum percentage change in fluorescence that scatter

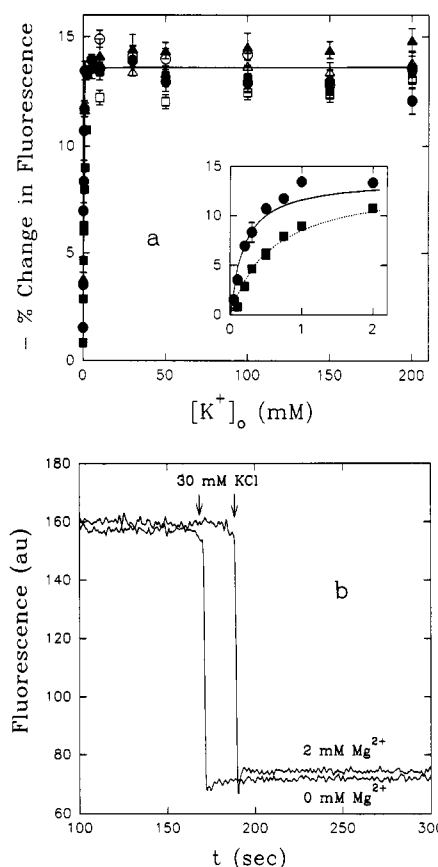


FIGURE 2: Effect of  $\text{Mg}^{2+}$  on amplitude of  $\text{K}^+$  quench for the same data set as in Figure 1. (a) Stopped-flow measurements. Minus the amplitude of the relaxation effect, expressed as percentage change in fluorescence ( $10^2 \Delta F_0/F$ ), is plotted against  $[\text{K}^+]_0$  at different  $\text{Mg}^{2+}$  concentrations. The meaning of the symbols is given in Figure 1. The theoretical curves through all of the points, which appear to be a single curve, were drawn with eq 8 and the parameter estimates in Table I. The inset shows the data for  $[\text{Mg}^{2+}]_0 = 0$  and 5 mM at low  $\text{K}^+$  concentrations on an expanded scale. The curves in the inset are the fit of the equation for a rectangular hyperbola to the amplitude data at 0 and 5 mM  $\text{Mg}^{2+}$ . The estimates of  $K_{0.5K}$  are 0.19 and 0.58 mM, respectively. (b) Equilibrium fluorescence measurements. Fluorescence in arbitrary units (au) is plotted versus time ( $t$ ). The lower trace resulted from mixing equal volumes of 60  $\mu\text{g mL}^{-1}$  protein and 60 mM KCl. In the experiment that resulted in the upper trace, the enzyme and titrant solutions also contained 2 mM  $\text{MgCl}_2$ . Both solutions were buffered by 50 mM Tris-HCl at pH = 7.4, and the ionic strength due to added salts was adjusted to  $\mu = 200$  mM with  $\text{ChoCl}$ . The temperature was ambient. The excitation wavelength was 495 nm, and the emission wavelength was 518 nm. The excitation and emission slit widths were both 2.5 mm. The solutions were mixed, and membrane fragments were kept in suspension, by stirring with a bar magnet.

randomly about  $13.6 \pm 0.7$ . The estimates of  $K_{0.5K}$  from the data at 0 and 5 mM  $\text{Mg}^{2+}$  are 0.19 and 0.58 mM, respectively. The apparent affinity of Na,K-ATPase for  $\text{K}^+$ , like the intrinsic affinity for  $\text{K}^+$  (Figure 1), decreases with increasing  $[\text{Mg}^{2+}]$ , but the magnitude of the fluorescence change at 15 °C is independent of  $[\text{Mg}^{2+}]$ . The maximum fluorescence change is also constant above 10 mM  $\text{K}^+$  and independent of  $[\text{Mg}^{2+}]$  at 8 and 22 °C.

Figure 2b demonstrates that the magnitude of the fluorescence change resulting from the  $\text{E}_1\text{K} \rightarrow \text{E}_2\text{K}$  transition is also independent of  $[\text{Mg}^{2+}]$  in steady-state experiments designed like stopped-flow experiments. That is, equal volumes of two solutions adjusted to the same pH and ionic strength were mixed in a conventional fluorometer. The lower trace resulted from mixing 60  $\mu\text{g mL}^{-1}$  Na,K-ATPase with 60 mM  $\text{K}^+$ , and the upper trace is the result of mixing enzyme

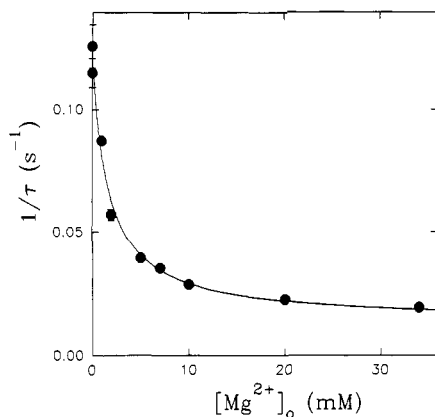


FIGURE 3: Effect of  $\text{Mg}^{2+}$  on  $1/\tau$  of  $\text{Na}^+$  reversal. Reciprocal relaxation times for the reversal of the  $\text{K}^+$  quench by  $\text{Na}^+$  are plotted against  $[\text{Mg}^{2+}]_0$ . Both syringes contained 5 mM  $\text{K}^+$ , the concentration of  $\text{Mg}^{2+}$  shown, and 50 mM Tris-HCl adjusted to pH = 7.4 at 15 °C. The enzyme syringe also contained 160  $\mu\text{g mL}^{-1}$  protein, 0.13 mM Tris-EDTA, and variable  $\text{ChoCl}$  for  $\mu = 200$  mM from added mono- and divalent cations. The ligand syringe contained 200 mM  $\text{NaCl}$ . Only at 0  $\text{Mg}^{2+}$  was the standard deviation, shown by vertical bars, bigger than the symbol size. The theoretical curve is the fit of eq 7 to the data. The parameter estimates are given in Table I.

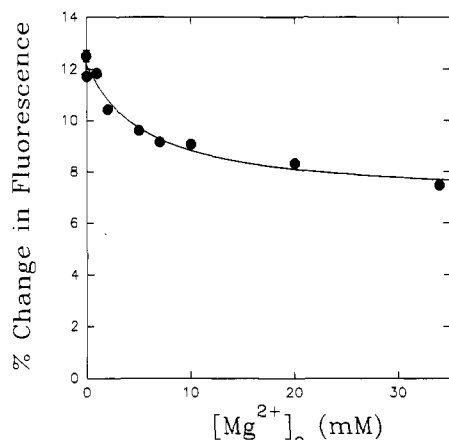


FIGURE 4: Effect of  $\text{Mg}^{2+}$  on amplitude of  $\text{Na}^+$  reversal. The amplitudes of the relaxation effects whose relaxation times are reported in Figure 3 are plotted as percentage change in fluorescence versus  $[\text{Mg}^{2+}]_0$ . The theoretical curve was calculated with eqs 11 and 31 and the following choice of parameters:  $k_f = 116 \text{ s}^{-1}$ ,  $k_r = 0.15 \text{ s}^{-1}$ ,  $k_{mf} = 99 \text{ s}^{-1}$ ,  $k_{mr} = 0.017 \text{ s}^{-1}$ ,  $K_{IK} = 15.1 \text{ mM}$ ,  $K_{IMK} = 287 \text{ mM}$ ,  $K_{IM} = 0.45 \text{ mM}$ ,  $K_{INa} = 0.044 \text{ mM}$ ,  $K_{IMNa} = 1.0 \text{ mM}$ , and  $\% \Delta F_{\text{max}}/F = 13.6$ .

preincubated in 2 mM  $\text{Mg}^{2+}$  with a solution containing 60 mM  $\text{K}^+$  and 2 mM  $\text{Mg}^{2+}$ . The effect of dilution was obtained by manually mixing enzyme solution with an equal volume of buffer and showed that the initial fluorescence intensity of the labeled enzyme with or without  $\text{Mg}^{2+}$  is exactly halved (not shown). The magnitude of the quench is 9.3%, both in the presence and in the absence of  $\text{Mg}^{2+}$ . In another experiment with a different labeled-enzyme preparation, the magnitude of the fluorescence quench with or without 5 mM  $\text{Mg}^{2+}$  was 11.4%.

**$1/\tau$  for  $\text{Na}^+$  Reversal.** Figure 3 is a scatter plot of  $1/\tau$  for reversal of the  $\text{K}^+$  quench by 100 mM  $\text{Na}^+$  versus  $[\text{Mg}^{2+}]$ . The value of  $1/\tau$  is inversely related to  $[\text{Mg}^{2+}]$  with half-maximum titrant concentration between 1 and 2 mM. We observed the same functional dependence of  $1/\tau$  on  $[\text{Mg}^{2+}]$  at 8 and 22 °C.

**Amplitude of  $\text{Na}^+$  Reversal.** Increasing  $[\text{Mg}^{2+}]$  also decreases the amplitude of the  $\text{Na}^+$ -reversal as illustrated in

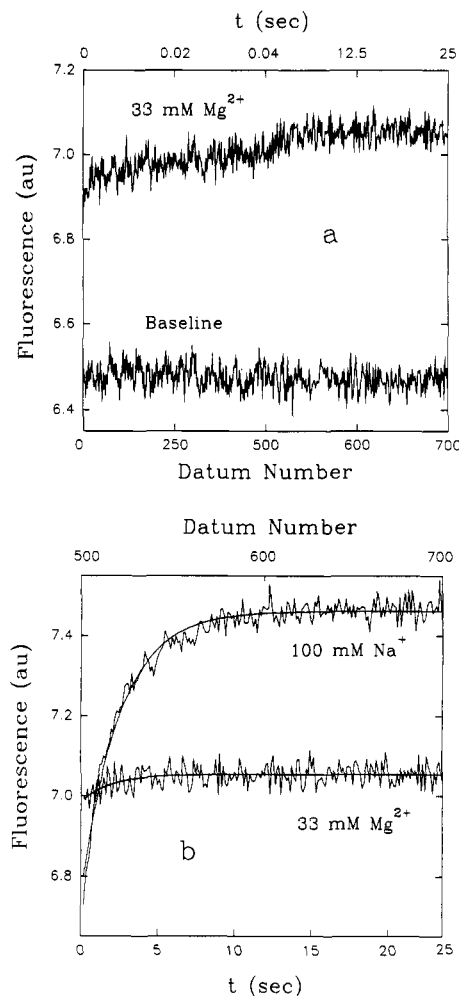


FIGURE 5: Reversal of  $\text{K}^+$  quench by  $\text{Mg}^{2+}$ . Fluorescence in arbitrary units is plotted against the datum number along one horizontal axis (top or bottom); the datum numbers are converted to time along the other horizontal axis. Each trace is the average of four experiments. (a) The enzyme syringe contained 160  $\mu\text{g mL}^{-1}$  protein, 0.13 mM Tris-EDTA, 5 mM KCl, and 200 mM  $\text{ChoCl}$  buffered by 50 mM Tris-HCl adjusted to pH = 7.4 at 22 °C. To obtain the lower trace, the enzyme was mixed with 5 mM KCl and 200 mM  $\text{ChoCl}$  in the same buffer. The upper trace resulted from replacing  $\text{ChoCl}$  with 66 mM  $\text{MgCl}_2$  in the titrant syringe. The rapid fluorescence enhancement must result from a process with half-time  $< t_d$ . (b) The data in the upper trace of part a is plotted on an expanded scale (lower trace) and compared to the reversal of the  $\text{K}^+$  quench obtained by replacing  $\text{MgCl}_2$  with 200 mM  $\text{NaCl}$  in the titrant syringe (upper trace). The smooth curves are the fits of a single exponential with offset to the data. The estimate of  $1/\tau$  for the slow effect caused by  $\text{Mg}^{2+}$  is  $0.52 \pm 0.16 \text{ s}^{-1}$ , and the estimate of amplitude is  $0.067 \pm 0.014 \text{ au}$ . For reversal of the  $\text{K}^+$  quench by  $\text{Na}^+$ ,  $1/\tau = 0.40 \pm 0.01 \text{ s}^{-1}$  and  $\Delta F_0 = 0.707 \pm 0.012 \text{ au}$ .

Figure 4. An inverse relationship between percentage change in fluorescence and  $[\text{Mg}^{2+}]$  was also found at 8 and 22 °C.

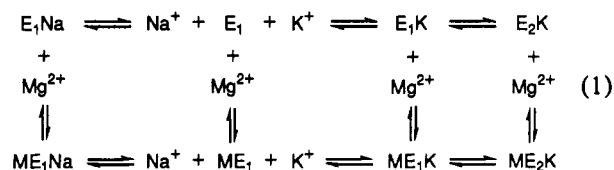
**$\text{Mg}^{2+}$  Reversal.**  $\text{Mg}^{2+}$  partially reverses the  $\text{K}^+$  quench. Figure 5a shows that the reaction is biphasic. The bottom trace is the baseline obtained by mixing enzyme in  $\text{K}^+$  with buffer. In the upper trace, enzyme preincubated with  $\text{K}^+$  was mixed with 66 mM  $\text{Mg}^{2+}$  without changing the photomultiplier high voltage. The display is split screen. That is, the sweep time for the first 500 data points was 30 ms, and 25 s was used to collect the next 200 data points. Most of the fluorescence enhancement is too fast to resolve in our stopped-flow instrument, approximately 85% of the increase in the first 500 data points occurring within the instrument dead time, or before collection of the first datum point.

Figure 5b shows data points 501–700 expanded and fitted to a single exponential with offset. The slower enhancement caused by  $\text{Mg}^{2+}$  (lower trace) is compared to reversal of the  $\text{K}^+$  quench by  $\text{Na}^+$  (upper trace). The estimated  $\tau$  for the slower reaction occurring in the second 200 data points is approximately the same as the  $\tau$  measured by reversing the  $\text{K}^+$  quench with  $\text{Na}^+$ , but the amplitude of the relaxation effect with  $\text{Mg}^{2+}$  is only about 1%. No fluorescence enhancement on the 25-s time scale could be detected with 5 or 10 mM final  $\text{Mg}^{2+}$  concentration.

## DISCUSSION

The effects of  $\text{Mg}^{2+}$  on the conformational change in Na,K-ATPase reported by fluorescein that are presented in the Results section can be summarized as follows: first,  $\text{Mg}^{2+}$  decreases the apparent affinity of the enzyme for  $\text{K}^+$  but does not affect the maximum rate of the  $\text{K}^+$ -quench; second, the amplitude of the  $\text{K}^+$  quench depends hyperbolically on the  $\text{K}^+$  concentration, approaching a maximum amplitude that is independent of the  $\text{Mg}^{2+}$  concentration; third, the rate at which  $\text{Na}^+$  reverses the  $\text{K}^+$  quench depends inversely on the  $\text{Mg}^{2+}$  concentration; and fourth, the amplitude of the  $\text{Na}^+$ -reversal also decreases with increasing  $\text{Mg}^{2+}$  concentration.

**Model for Specific Interaction of  $\text{Mg}^{2+}$  with Dephosphoenzyme.** To explain these experimental observations, we propose a general model in which  $\text{Mg}^{2+}$  binds at a different site than  $\text{Na}^+$  and  $\text{K}^+$  but may affect the rate constants for the  $\text{E}_1 \rightleftharpoons \text{E}_2$  conformational change, as well as the affinity of the enzyme for monovalent cations. The mechanism can be written



with forward defined as from left to right, which gives

$$1/\tau = k_f \chi_{\text{E}_1\text{K}} + k_{\text{mr}} \chi_{\text{ME}_1\text{K}} + k_r \chi_{\text{E}_2\text{K}} + k_{\text{mr}} \chi_{\text{ME}_2\text{K}} \quad (2)$$

where

$$\chi_{\text{E}_1\text{K}} = [\text{K}^+]_0 / \left\{ [\text{K}^+]_0 \left( 1 + \frac{[\text{Mg}^{2+}]_0}{K_{1\text{MNa}}} \right) + K_{1\text{K}}(\text{app}) \left[ 1 + [\text{Mg}^{2+}]_0 \left( 1 + \frac{[\text{Na}^+]_0}{K_{1\text{MNa}}} \right) / K_{1\text{M}} \left( 1 + \frac{[\text{Na}^+]_0}{K_{1\text{Na}}} \right) \right] \right\} \quad (3)$$

$$\chi_{\text{ME}_1\text{K}} = [\text{K}^+]_0 / \left\{ [\text{K}^+]_0 \left( 1 + \frac{K_{1\text{KM}}}{[\text{Mg}^{2+}]_0} \right) + K_{1\text{MK}}(\text{app}) \left[ 1 + K_{1\text{M}} \left( 1 + \frac{[\text{Na}^+]_0}{K_{1\text{Na}}} \right) / [\text{Mg}^{2+}]_0 \left( 1 + \frac{[\text{Na}^+]_0}{K_{1\text{MNa}}} \right) \right] \right\} \quad (4)$$

and

$$\chi_{\text{E}_2\text{K}} = \frac{K_{2\text{KM}}}{([\text{Mg}^{2+}]_0 + K_{2\text{KM}})} \quad \chi_{\text{ME}_2\text{K}} = \frac{[\text{Mg}^{2+}]_0}{([\text{Mg}^{2+}]_0 + K_{2\text{KM}})} \quad (5)$$

The notation is explained in the Appendix.

Table I: Summary of Derived Rate and Equilibrium Constants<sup>a</sup>

const	temp (°C)				method
	8	15	22		
			exptl	lit.	
$k_f = k_{\text{mf}}$	$65 \pm 2$	$142 \pm 2$	$344 \pm 7$	320	est. from $\text{K}^+$ quench (eq 2)
$K_{1\text{M}}$	$0.42 \pm 0.09$	$0.31 \pm 0.04$	$0.16 \pm 0.02$		
$K_{1\text{K}}$	$10.3 \pm 1.4$	$12.6 \pm 1.1$	$14.3 \pm 1.4$	10	
$K_{1\text{MK}}$	$298 \pm 90$	$223 \pm 27$	$206 \pm 19$		
$10^2 k_r$	$2.13 \pm 0.03$	$12.1 \pm 0.3$	$38.4 \pm 0.3$	44	est. from $\text{Na}^+$ reversal (eq 7)
$10^2 k_{\text{mr}}$	$0.56 \pm 0.03$	$1.4 \pm 0.4$	$6.1 \pm 0.3$		
$K_{2\text{KM}}$	$2.8 \pm 0.3$	$1.7 \pm 0.3$	$2.8 \pm 0.1$		
$10^2 K_{1\text{Na}}$	4.7	4.4	10	19	fit rev. ampl. (eqs 11 and 31)
$K_{1\text{MNa}}$	8.9	1.0	3.3		
$10^{-2} K_c$	$16.5 \pm 3.1$	$10.7 \pm 2.0$	$7.1 \pm 1.3$	7	calc from est. consts
$10^{-2} K_{\text{mc}}$	$112 \pm 22$	$81 \pm 16$	$59 \pm 12$		
$K_{1\text{KM}}$	$12.1 \pm 7.9$	$5.5 \pm 1.8$	$2.3 \pm 0.7$		

<sup>a</sup>  $k$  denotes a rate constant in  $\text{s}^{-1}$ , and  $K$  designates an equilibrium dissociation constant in mM units.  $\mu = 200$  mM from added salt in 50 mM Tris-HCl buffer at pH 7.4. Literature (lit.) refers to Faller et al. (1991a). Fit means that the data are compatible with the quoted value (see text).

If  $[\text{Na}^+] = 0$ ,  $k_f = k_{\text{mf}}$ , and  $k_r = k_{\text{mr}}$ , eq 2 reduces to

$$\frac{1}{\tau} = k_f \left[ \frac{[\text{K}^+]_0}{[\text{K}^+]_0 + K_{1\text{K}} \left( 1 + \frac{[\text{Mg}^{2+}]_0}{K_{1\text{KM}}} \right)} \right] + k_r \quad (6)$$

The second term in the denominator of the bracket quantity in eq 6 is the  $\text{K}^+$  concentration at which  $1/\tau \approx k_f/2$ . The half-maximum  $[\text{K}^+]$  increases from  $K_{1\text{K}}$  when  $[\text{Mg}^{2+}] = 0$  to  $K_{1\text{MK}}$  when  $[\text{Mg}^{2+}]$  approaches infinity, and the upper pathway in eq 1 can be ignored (Appendix, eq 29). Initial estimates of  $K_{1\text{K}} = 10.2$  mM,  $K_{1\text{M}} = 0.26$  mM, and  $K_{1\text{KM}} = 7.3$  mM were obtained by fitting the analytical expression for the half-maximum  $[\text{K}^+]$  in eq 6 to the estimates of  $K_{\text{K}}$  as a function of  $[\text{Mg}^{2+}]$  obtained from the data in Figure 1 with eq 4 in Faller et al. (1991a) as explained in the Results section.

We have previously shown that  $1/\tau$  is inversely related to  $[\text{Na}^+]$  and extrapolates to  $k_{-2}$  at high  $[\text{Na}^+]$  (Faller et al., 1991a). At sufficiently high  $\text{Na}^+$  concentrations in the presence of  $\text{Mg}^{2+}$ , the first two terms in eq 2 can be neglected and the reciprocal relaxation time becomes

$$\frac{1}{\tau} = k_r \left( \frac{K_{2\text{KM}}}{[\text{Mg}^{2+}]_0 + K_{2\text{KM}}} \right) + k_{\text{mr}} \left( \frac{[\text{Mg}^{2+}]_0}{[\text{Mg}^{2+}]_0 + K_{2\text{KM}}} \right) \quad (7)$$

In support of equating the  $1/\tau$  values obtained by reversing the  $\text{K}^+$  quench with 100 mM  $\text{Na}^+$  in the presence of varying concentrations of  $\text{Mg}^{2+}$  to the expression for  $1/\tau$  in eq 7, experimentally indistinguishable values of  $1/\tau$  were measured at 0 and 10 mM  $\text{Mg}^{2+}$  when the  $\text{K}^+$  quench was reversed by 200 mM  $\text{Na}^+$ , and the value of  $1/\tau$  at 0  $\text{Mg}^{2+}$  is in good agreement with the value of  $k_{-2} = 0.16 \text{ s}^{-1}$  that we estimated from a plot of  $1/\tau$  versus  $[\text{Na}^+]$  at 15 °C (Faller et al., 1991a). Estimates of  $k_r = 0.12 \text{ s}^{-1}$ ,  $k_{\text{mr}} = 0.014 \text{ s}^{-1}$ , and  $K_{2\text{KM}} = 1.7$  mM were obtained by fitting eq 7 to the data in Figure 3. The solid line in Figure 3 is the calculated curve.

Reciprocal relaxation times showing the same dependence on  $[\text{Mg}^{2+}]$  were measured in both  $\text{K}^+$ -quench and  $\text{Na}^+$ -reversal experiments at 8 and 22 °C. The estimates of the reverse rate constants and  $K_{2\text{KM}}$  obtained by fitting eq 7 to  $\text{Na}^+$ -reversal data are recorded in Table I. Best estimates of  $k_f = k_{\text{mf}}$ ,  $K_{1\text{K}}$ ,

Table II: Derived Thermodynamic Parameters<sup>a</sup>

const	$E_a$ (kcal mol <sup>-1</sup> )	$\Delta H^*$ (kcal mol <sup>-1</sup> )	$\Delta G^*$ (kcal mol <sup>-1</sup> )	$\Delta S^*$ (eu)
$k_f = k_{mf}$	20.5 ± 1.9	19.8 ± 1.9	13.9 ± 0.3	20.0 ± 7.5
$k_r$	30.3 ± 2.9	29.6 ± 2.9	17.7 ± 0.0	40.3 ± 9.8
$k_{mr}$	28.0 ± 4.6	27.4 ± 4.6	18.9 ± 0.1	28.8 ± 15.9
$K_c$		-9.8 ± 4.8	-3.8 ± 0.3	-20.3 ± 17.3
$K_{mc}$		-7.6 ± 6.5	-5.0 ± 0.1	-8.8 ± 23.4
$K_{IM}$		-11.4 ± 2.6	5.1 ± 0.2	-55.9 ± 9.5
$K_{IK}$		3.9 ± 0.4	2.5 ± 0.1	4.7 ± 1.7
$K_{IKM}$		-19.6 ± 0.8	3.6 ± 0.4	-78.6 ± 4.1

<sup>a</sup> Estimate ± SD.  $\Delta G^*$  and  $\Delta S^*$  at 22 °C. The asterisk represents \* for quasi-thermodynamic activation parameters derived from rate constants ( $k$ ) and ° for standard energy changes derived from equilibrium constants ( $K$ ).

$K_{IM}$ , and  $K_{IMK}$  at each temperature were obtained by fitting the first two terms in eq 2 with  $[Na^+] = 0$  to the combined  $K^+$ -quench data at all  $Mg^{2+}$  concentrations.  $k_f$  and  $k_{mr}$  were set equal to 0, because the ordinate intercept in  $K^+$ -quench experiments with the Na,K-ATPase is 0 within experimental error. The justification for setting  $k_f = k_{mf}$  is that five parameter fits of eq 2, minus the reversal terms in eq 7, to the  $K^+$ -quench data gave numerically indistinguishable estimates of the forward rate constants (e.g.,  $k_f = 143 \pm 3$  and  $k_{mf} = 139 \pm 20$  at 15 °C). The directly estimated parameters, together with parameters derived from them by equating alternative pathways (Appendix, eq 29), are summarized in Table I. The standard energy changes calculated from the equilibrium dissociation constants that showed a monotonic change with temperature are reported in Table II. The tabulated estimates of the activation energies are improved values obtained by combining the estimates of the rate constants in Table I with those published earlier (Faller et al., 1991a; Table I) and analyzing them with Eyring's transition-state theory (Frost & Pearson, 1953). The standard energy changes reported for the conformational change are the difference between the forward and the reverse activation parameter, with the large uncertainties resulting from propagation of errors.

Assuming that a single reaction is being observed in both experiments, the maximum fluorescence change, or amplitude, estimated from a stopped-flow trace contains the same information as an equilibrium titration in a conventional fluorometer. The equation derived for the amplitude of a  $K^+$ -quench experiment from the mechanism in eq 1,

$$\frac{\Delta F_o}{F} = \left[ \frac{[K^+]_o}{[K^+]_o + K_{0.5(M)K}} \right] A_{(M)K} \frac{\Delta F_{max}}{F} \quad (8)$$

predicts hyperbolic dependence upon  $[K^+]$  at each  $[Mg^{2+}]$  with half-maximum  $[K^+]$

$$K_{0.5(M)K} = \left[ \frac{K_{0.5K} K_{0.5MK} (K_{IM} + [Mg^{2+}]_o)}{K_{0.5MK} K_{IM} + K_{0.5K} [Mg^{2+}]_o} \right] \quad (9)$$

and a maximum, relative fluorescence change ( $\Delta F_{max}/F$ ) reduced by the amplitude factor

$$A_{(M)K} = \frac{K_{0.5MK} K_{IM} A_c + K_{0.5K} [Mg^{2+}]_o A_{mc}}{K_{0.5MK} K_{IM} + K_{0.5K} [Mg^{2+}]_o} \quad (10)$$

The curves  $0 \leq [K^+] \leq 2$  mM in the inset of Figure 2a are best fits of the equation for a rectangular hyperbola to the  $[Mg^{2+}] = 0$  and  $[Mg^{2+}] = 5$  mM data. The maxima estimated in this way are equivalent to estimates of  $\Delta F_{max}/F$ , because  $k_f \gg k_r$  and  $k_{mf} \gg k_{mr}$  for the sodium pump (Table I), so that

$A_{(M)K} \approx 1$ . The theoretical line  $5 \leq [K^+] \leq 200$  mM in Figure 2a was drawn by substituting the mean value of  $\Delta F_{max}/F$  quoted in the Results section and the values of the other parameters given in Table I into eq 8.

The amplitude of  $Na^+$  reversals of the  $K^+$  quench as a function of  $[Mg^{2+}]$  at fixed  $[K^+]$  depends on the fraction of the enzyme in the  $E_1$  conformation ( $\chi_1$ ) before ( $[Na^+] = 0$ ) and after ( $[Na^+] = 100$  mM) mixing with  $Na^+$  (eq 31). Choosing  $Mg^{2+}$  as the independent variable,

$$\chi_1 = \left( \frac{[Mg^{2+}]_o}{[Mg^{2+}]_o + K_{0.5(Na)M}} + \frac{\text{const}}{[Mg^{2+}]_o + K_{0.5(Na)M}} \right) A_{(Na)M} \quad (11)$$

where

$$\text{const} = K_{IM} \left( \frac{1 + \frac{[K^+]_o}{K_{IK}} + \frac{[Na^+]_o}{K_{INa}}}{1 + \frac{[K^+]_o}{K_{IMK}} + \frac{[Na^+]_o}{K_{IMNa}}} \right) \quad (12)$$

$$A_{(Na)M} = \frac{\left( 1 + \frac{[K^+]_o}{K_{IMK}} + \frac{[Na^+]_o}{K_{IMNa}} \right)}{\left( 1 + \frac{[K^+]_o}{K_{0.5MK}} + \frac{[Na^+]_o}{K_{IMNa}} \right)} \quad (13)$$

and

$$K_{0.5(Na)M} = K_{IM} \left( \frac{1 + \frac{[K^+]_o}{K_{0.5K}} + \frac{[Na^+]_o}{K_{INa}}}{1 + \frac{[K^+]_o}{K_{0.5MK}} + \frac{[Na^+]_o}{K_{IMNa}}} \right) \quad (14)$$

Hyperbolic dependence of relative fluorescence on  $[Mg^{2+}]$  is predicted and observed experimentally with empirical half-maximum  $[Mg^{2+}]$  given by eq 14. Equation 11 substituted into eq 31 cannot be used to estimate parameters for two reasons. First, the number of parameters approaches the number of experimental points, and second, the parameters are highly correlated, because all of the parameters that occur in the amplitude factor (eq 13) also appear in the half-maximum expression (eq 14). What can be done is show that eq 31, evaluated with the help of eq 11, fits the experimental data with reasonable choices of the parameters. The theoretical curve in Figure 4 demonstrates that the experimental data at 15 °C can be fit without any parameter differing from the estimates in Table I, or in the case of  $K_{INa}$  from the earlier estimate (Faller et al., 1991a), by more than 50% and with  $\Delta F_{max}/F$  equal to the median value observed in quench experiments (13.6%). Comparable agreement between the parameter estimates in Table I and values that fit eqs 11 and 31 to the experimental data is possible at 8 and 22 °C.

Equation 11 with  $[Na^+] = 0$  and eq 31 can be used to predict whether reversal of the  $K^+$  quench by  $Mg^{2+}$  should be observed. Approximately 1% reversal of a 5 mM  $K^+$  quench by 33 mM  $Mg^{2+}$  is predicted by substituting the parameter estimates in Table I into eqs 11 and 31. In qualitative agreement with this prediction, the estimated amplitude of the slower,  $Mg^{2+}$ -caused fluorescence enhancement in Figure 5 is about 7% of the reversal observed with  $Na^+$ .

**Internal Consistency of Model.** The theoretical curves in Figures 1–4 were calculated by substituting the parameter estimates in Table I into eqs 2–14 derived for the mechanism proposed in eq 1. The excellent agreement between theory

and experiment at 15 °C demonstrates that the model can explain the functional dependence of  $1/\tau$  for the  $\text{K}^+$ -quench reaction on monovalent and divalent cation concentrations (Figure 1), the increase in half-maximum  $\text{K}^+$  concentration with  $\text{Mg}^{2+}$  concentration (Figure 1), the independence of the maximum fluorescence change from  $\text{Mg}^{2+}$  concentration at saturating  $\text{K}^+$  concentrations (Figure 2), and the inverse relationship between  $\text{Mg}^{2+}$  concentration and both  $1/\tau$  (Figure 3) and percentage fluorescence change (Figure 4) for the  $\text{Na}^+$ -reversal reaction. Data at 8 and 22 °C are in comparable agreement with the predictions of the model.

The parameters estimated previously for apoenzyme (Faller et al., 1991a) are included in Table I for comparison with the values obtained from studying the metalloenzyme. The earlier values of  $k_r$  and  $K_{1\text{Na}}$  are independent estimates, because they were derived from plots of  $1/\tau$  versus  $[\text{Na}^+]$  instead of  $[\text{Mg}^{2+}]$ . The estimates of  $k_f$  and  $K_{1\text{K}}$  are also independent, because values of  $k_f$  and  $K_{1\text{K}}$  close to the estimates in Table I are obtained if the  $[\text{Mg}^{2+}] = 0$  points in Figure 1 are omitted and eqs 2–14 are fitted only to the  $[\text{Mg}^{2+}] \neq 0$  data.

The most compelling evidence that the model in eq 1 provides a consistent interpretation of both  $\text{K}^+$ -quench and  $\text{Na}^+$ -reversal experiments as a function of  $[\text{Mg}^{2+}]$  is that the value of  $K_{2\text{KM}}$  calculated from the  $\text{K}^+$ -quench estimates of  $K_{1\text{KM}}$  and  $k_f = k_{\text{mf}}$  and the  $\text{Na}^+$ -reversal estimates of  $k_r$  and  $k_{\text{mr}}$  at 15 °C in Table I,

$$K_{2\text{KM}} = K_{1\text{KM}} \frac{K_c}{K_{\text{mc}}} = K_{1\text{KM}} \frac{k_f k_{\text{mr}}}{k_{\text{mf}} k_r} = 0.7 \pm 0.5 \text{ mM} \quad (15)$$

is in reasonable agreement with the estimate of  $K_{2\text{KM}} = 1.7 \pm 0.3 \text{ mM}$  obtained directly from  $\text{Na}^+$ -reversal experiments. The calculated value of  $K_{2\text{KM}}$  is an independent estimate even though it involves  $k_r$  and  $k_{\text{mr}}$ , because the reverse rate constants could be obtained from just two  $\text{Na}^+$ -reversal measurements, at 0 and saturating  $\text{Mg}^{2+}$  concentrations, without any knowledge of the shape of the  $1/\tau$  versus  $[\text{Mg}^{2+}]$  curve which determines  $K_{2\text{KM}}$ . The indirectly calculated and directly estimated values of  $K_{2\text{KM}}$  are also in satisfactory agreement at 8 and 22 °C.

There is one inconsistency between the predictions of the model and the experimental data that we have noted previously (Faller et al., 1991a,b). Substituting the parameter values in Table I into eq 9 gives "kinetic" estimates of the half-maximum for the amplitude of the  $\text{K}^+$  quench of 0.012 mM at 0  $\text{Mg}^{2+}$  and 0.027 mM at 5 mM  $\text{Mg}^{2+}$ , compared with equilibrium estimates which were used to draw the theoretical curves shown in the inset to Figure 2a of 0.19 to 0.58 mM at 0 and 5 mM  $\text{Mg}^{2+}$ , respectively. An order of magnitude, or more, difference between kinetic and equilibrium estimates of  $K_{0.5\text{K}}$  was reported in the original paper proposing the top line in eq 1 to explain how  $\text{Na}^+$  and  $\text{K}^+$  cause the conformational change reported by fluorescein (Karlsh, 1980) and has been confirmed by us (Faller et al., 1991b; Table I). This discrepancy is important, because it implies that the model in eq 1 is not a complete description of the reaction reported by fluorescein. However, the problem is not with the expansion of the model to include  $\text{Mg}^{2+}$ 's effects, and therefore an explanation of the discrepancy is deferred to a paper in preparation.

**Comparison of Parameter Estimates to Literature Values.** Our results confirm the discovery made by Hegyvary and Jorgensen (1981) that  $\text{Mg}^{2+}$  reduces the rate of the  $\text{Na}^+$ -reversal reaction. The agreement is quantitative. The mean of our estimates of  $K_{2\text{KM}}$  is  $2.3 \pm 0.8 \text{ mM}$  compared with the value they quote (1.2 mM). The "puzzling difference between their results" and reverse rates reported at lower temperatures

(Glynn, 1985) is only apparent. Correcting our estimates of  $k_r$  and  $k_{\text{mr}}$  in Table I at 22 to 25 °C with the Arrhenius activation energies ( $E_a$ ) quoted in Table II, and remembering that Hegyvary and Jorgensen measured first-order time constants or relaxation times rather than rate constants, gives, with the help of eq 2,  $1/\tau = 1.4 \text{ s}^{-1}$  when  $[\text{Mg}^{2+}] = 0$ , and  $1/\tau = 0.7 \text{ s}^{-1}$  when  $[\text{Mg}^{2+}] = 4 \text{ mM}$ , at 25 °C and 10 mM  $\text{K}^+$ , compared with values in Figure 4 of their paper of 1.7  $\text{s}^{-1}$  and 0.4  $\text{s}^{-1}$ , respectively.

**$K_d$  and  $\Delta H^\circ$  for  $\text{Mg}^{2+}$  Binding.** Published values of the dissociation constant ( $K_d$ ) for  $\text{Mg}^{2+}$  from  $\text{Na,K-ATPase}$  range from 0.15 to 1 mM, in good agreement with the range  $0.16 \leq K_d \leq 2.3 \text{ mM}$  obtained in this study at 22 °C, depending upon the enzyme conformation and whether  $\text{K}^+$  or  $\text{Na}^+$  is bound.

$K_d$ 's estimated from measurements in the absence of  $\text{K}^+$  cluster near the lower end of the range and approximate our value of  $K_{1\text{M}} = 0.16 \text{ mM}$ . Thermal titration, which is the most direct method, gave  $K_d = 0.83 \text{ mM}$  (Kuriki et al., 1976). A  $K_d$  of 0.25 mM has been evaluated from  $\text{Mg}^{2+}$ -induced shifts in the fluorescence of bound versus free eosin (Skou & Esmann, 1983). EPR measurements give  $K_d = 0.15 \text{ mM}$  for  $\text{Mg}^{2+}$  dissociation from apoenzyme (Grisham & Mildvan, 1974). The last value is particularly important, because it is deduced from competition between  $\text{Mg}^{2+}$  and  $\text{Mn}^{2+}$  for a site to which  $\text{Mn}^{2+}$  binds immeasurably tightly ( $K_d < 0.74 \mu\text{M}$ ). The stoichiometry of  $\text{Mn}^{2+}$  binding with high affinity is 1. Distances from this  $\text{Mn}^{2+}$  to inorganic phosphate (Grisham & Mildvan, 1975), CrATP (O'Conner & Grisham, 1980), and CoATP (Stewart & Grisham, 1988) that are consistent with the enzyme-bound divalent cation participating directly in the hydrolysis-hydration reaction as an electrophilic catalyst have been measured by EPR,  $^1\text{H}$  NMR, and  $^{31}\text{P}$  NMR.

$K_d$ 's for  $\text{Mg}^{2+}$  measured in the presence of  $\text{K}^+$  are higher, approximating our mean estimate of  $K_{2\text{KM}} = 2.3 \text{ mM}$ . The value deduced from competition between  $\text{Mg}^{2+}$  and  $\text{Mn}^{2+}$  in the presence of 100 mM  $\text{Na}^+$  and 10 mM  $\text{K}^+$ , conditions approaching ours, was 1 mM (Grisham & Mildvan, 1974). Both this  $K_d$  value for  $\text{Mg}^{2+}$  and  $K_d < 0.98 \mu\text{M}$  for  $\text{Mn}^{2+}$  in the presence of assay concentrations of  $\text{Na}^+$  and  $\text{K}^+$  agree with kinetically determined activation constants of 0.9 mM for  $\text{Mg}^{2+}$  (Rendi & Uhr, 1964) and 0.88  $\mu\text{M}$  for  $\text{Mn}^{2+}$  (Grisham & Mildvan, 1974). Numerical agreement between the  $\text{Mg}^{2+}$  dissociation constants in Table I and values derived from competition between  $\text{Mg}^{2+}$  and the  $\text{Mn}^{2+}$  that has been used to map the active site is strong evidence that the  $\text{Mg}^{2+}$  that affects the conformational change reported by fluorescein is the divalent cation required for catalytic activity.

The thermodynamic parameters calculated from the temperature dependence of  $K_{1\text{M}}$  and recorded in Table II are interesting, because they indicate that  $\text{Mg}^{2+}$  binding to the enzyme is exergonic, even though the reaction is endothermic ( $\Delta H^\circ = 11.4 \text{ kcal mol}^{-1}$ ), and therefore  $\text{Mg}^{2+}$  binding must be entropy driven. Although this result might seem surprising, it is consistent with calorimetric studies of divalent cation binding to other proteins (Henkens et al., 1968). The enthalpy of binding of  $\text{Mg}^{2+}$  to  $\text{Na,K-ATPase}$  is in remarkable numerical agreement with the enthalpy of binding of  $\text{Mg}^{2+}$  to another  $\text{Mg}^{2+}$ -activated enzyme, enolase ( $\Delta H^\circ = 11.7 \text{ kcal mol}^{-1}$ ), which the author measured by flow microcalorimetry (Faller & Johnson, 1974). Robinson (1989) has concluded from a larger effect of DMSO than of temperature on  $K_d$  for  $\text{Mg}^{2+}$  activation of pNPPase activity that  $\text{Mg}^{2+}$  binding to  $\text{Na,K-ATPase}$  is entropy driven. One plausible explanation of the temperature dependence of  $K_{1\text{M}}$  is that binding to the



enzyme reduces the hydration number of  $\text{Mg}^{2+}$ .

**$K_d$  for Monovalent Cation Binding.** Extrapolation to 0  $\text{Mg}^{2+}$  gives an estimate of  $K_{1K}$  (Table I) for dissociation of  $\text{K}^+$  from apoE<sub>1</sub> that is in excellent quantitative agreement with the value (9 mM) deduced from measurements of Na efflux from red blood cells by assuming that  $\text{K}^+$  and  $\text{Na}^+$  bind competitively to an intracellular site (Garay & Garrahan, 1973).  $K_{1Na}$  (Table I), the  $\text{Na}^+$  dissociation constant from apoE<sub>1</sub> that is consistent with our  $\text{Mg}^{2+}$  model (eq 1), is also in satisfactory agreement with the value that was estimated from  $\text{Na}^+$  efflux measurements (0.19 mM).

$\text{Mg}^{2+}$  binding reduces the affinity of the E<sub>1</sub> conformer for  $\text{K}^+$  ( $K_{1MK}$ ) more than an order of magnitude (Table I). There are two precedents in the literature for  $\text{K}^+$  binding to E<sub>1</sub> with such a low affinity in functional assays. In the first, Robinson (1975) studied  $\text{K}^+$  inhibition of pNPPase activity. He concluded that  $\text{K}^+$  acts as a noncompetitive inhibitor by occupying the discharge site for the monovalent cation transported into the cell. The value of  $K_d$  that he estimated for dissociation of  $\text{K}^+$  from this intracellular site was 140 mM. The second precedent for low-affinity  $\text{K}^+$  binding is also contained in a paper by Robinson (Robinson et al., 1977). To determine the affinity of  $\text{K}^+$  at its intracellular discharge site, the sodium pump was reversed, and the rate of ATP synthesis in resealed red blood cell ghosts was measured as a function of internal  $\text{K}^+$  concentration. The results were interpreted as evidence for  $\text{K}^+$  binding with  $K_{0.5} = 297$  mM.  $\text{Mg}^{2+}$  was present in both of Robinson's experiments, and our estimates of  $K_{1MK}$  (Table I) fall between the values Robinson attributes to  $\text{K}^+$  dissociation from an intracellular  $\text{K}^+$  discharge site.

Numerical agreement between published  $\text{K}^+$  dissociation constants and the estimates of  $K_{1K}$  and  $K_{1MK}$  in Table I certainly supports the model in eq 1, but numerical comparisons must be interpreted cautiously for two reasons. First, the agreement is not as good as it appears. The problem is that different experimental conditions were used in making the measurements that are being compared. For example, Robinson's experiments were carried out at 37 °C. Using the rough estimate of  $\Delta H^\circ$  that can be made from the values of  $K_{1MK}$  in Table II to correct his pNPPase inhibition constant at 37 °C (140 mM) to 22 °C gives a value (200 mM) even closer to our estimate of  $K_{1MK}$  at 22 °C (223 mM), but applying the same temperature correction to the constant for  $\text{K}^+$  activation of ATP synthesis at 37 °C gives poorer agreement (424 mM). The cumulative difference between published values and our estimates of the  $\text{Na}^+$  and  $\text{K}^+$  dissociation constants after correction for temperature, ionic strength, etc., could easily be as much as 3–5-fold. Second, the reasoning in the comparisons is *a posteriori*.  $\text{Na}^+$  efflux is also measured in the presence of  $\text{Mg}^{2+}$  (Garay & Garrahan, 1973). The only justification for comparing the  $\text{K}^+$  dissociation constant derived from  $\text{Na}^+$  efflux measurements with  $K_{1K}$  for dissociation from apoenzyme and the  $K_d$ 's inferred from pNPPase inhibition and activation of ATP synthesis with  $K_{1MK}$  for dissociation from metalloenzyme is that numerical agreement is obtained. Therefore, it is important that our model also gives estimates of  $\text{Mg}^{2+}$  dissociation constants consistent with published values and an enthalpy of  $\text{Mg}^{2+}$  binding for which there is precedent and that eq 1 provides a simpler explanation of  $\text{Mg}^{2+}$ 's effects on the  $\text{E}_1 \rightleftharpoons \text{E}_2$  conformational change than postulating a different conformation of the metalloenzyme.

**Explanation of Discrepancies with Published Data.** Although the dissociation constants are in satisfactory agreement, our estimate of the heat of  $\text{Mg}^{2+}$  binding to Na,K-ATPase

from the temperature dependence of  $K_{1M}$  (11.4 kcal mol<sup>-1</sup>) does not agree with the published microcalorimetric measurement. An "extraordinarily large" exothermic enthalpy of  $\text{Mg}^{2+}$  binding (–49 kcal mol<sup>-1</sup>) was interpreted as evidence for a metal-induced conformational change in the enzyme (Kuriki et al., 1976). The discrepancy between the van't Hoff and calorimetric enthalpies of binding may be only apparent. The advantage of calorimetric measurements is that binding of optically silent metals like  $\text{Mg}^{2+}$  can be followed. The disadvantage is that the measured heat is the resultant of all of the chemical reactions that occur. Whether the reaction of  $\text{Mg}^{2+}$  with enolase was endothermic or exothermic depended upon the heat of ionization of the buffer (Faller & Johnson, 1974a). The explanation was that two protons are released when  $\text{Mg}^{2+}$  binds to the enzyme (Faller & Johnson, 1974b). The binding of  $\text{Mg}^{2+}$  to Na,K-ATPase was measured in only one buffer, imidazole, which has a large heat of ionization equal to 8.8 kcal mol<sup>-1</sup> (Wadsö, 1962). The stoichiometry of  $\text{Mg}^{2+}$  binding under the experimental conditions used in the calorimetric measurements was not determined. Therefore, alternative explanations of the published thermal titration of Na,K-ATPase with  $\text{Mg}^{2+}$  are possible.

The fundamental differences between our experimental results and previously published titrations of FITC-labeled Na,K-ATPase with  $\text{Mg}^{2+}$  present are that the magnitude of the fluorescence quench was independent of  $\text{Mg}^{2+}$  concentration (Figure 2) and  $\text{Mg}^{2+}$  caused only a small reversal of the  $\text{K}^+$  quench (Figure 5b). Therefore, we are able to explain the effects of  $\text{Mg}^{2+}$  on the conformational change in the Na,K-ATPase reported by fluorescein without introducing a different, fluorometrically-detectable conformation of the metalloenzyme. The reason for the apparent discrepancy is that conventional fluorescence titrations measure the resultant of all the changes in emission intensity that occur during an experiment, just as calorimetric measurements report the resultant of all the heat changes associated with a reaction. Some of the changes in fluorescence emission intensity that contribute to equilibrium measurements are not specific for  $\text{Mg}^{2+}$ ,  $\text{K}^+$ , or  $\text{Na}^+$  (Grell et al., 1991). A stopped-flow study in which these effects are time-resolved and interpreted as in preparation. Here we show that stopped-flow and equilibrium fluorescence measurements give the same results.

Approximately 50% reversal of the  $\text{K}^+$  quench by  $\text{Mg}^{2+}$  has been reported (Karlsh, 1980; Hegyvary & Jorgensen, 1981). Our model predicts only about 1% reversal of the conformational change. Figure 5 shows that both the published experimental observations and the prediction of our model are correct. When  $\text{Mg}^{2+}$  is mixed with enzyme quenched by  $\text{K}^+$ , there is a fluorescence enhancement that is too fast to resolve in the stopped-flow instrument (faster sweep time on the left in Figure 5a) and probably not caused by a protein conformational change. Grell et al. (1992) have independently concluded that not all of the fluorescence changes reported by fluorescein result from the  $\text{E}_1 \rightleftharpoons \text{E}_2$  conformational change. Subsequently, there is a slow fluorescence enhancement on the time scale of the increase in fluorescence intensity caused by  $\text{Na}^+$  in the absence of  $\text{Mg}^{2+}$  (slower sweep time on the right in Figure 5a and Figure 5b). Our model (eq 1) explains only the slow effect that yields estimates of  $\text{Mg}^{2+}$  and  $\text{K}^+$  dissociation constants consistent with values observed in functional catalysis and transport assays.

Preincubation with  $\text{Mg}^{2+}$  reportedly reduces the magnitude of the  $\text{K}^+$  quench observed in conventional, equilibrium fluorescence measurements (Karlsh, 1980; Hegyvary & Jorgensen, 1981). Preincubation with greater than 2 mM



$Mg^{2+}$  does not affect the amplitude of the fluorescence quench observed in stopped-flow measurements (Figure 2a). We are able to reproduce the observations from other laboratories, qualitatively at least, if we copy their experimental protocols. However, ionic strength was not kept constant in the published titrations, and errors accumulate when aliquots of titrant are added successively. If the 50 mM  $K^+$  point is omitted, the  $[Mg^{2+}] = 0, 0.2,$  and  $2.1$  mM curves in Figure 2 of the Hegyvary and Jorgensen paper all extrapolate to the same maximum fluorescence change ( $132 \pm 3$  au). Figure 2b shows that if equal volumes are mixed in a steady-state fluorometer, so that there is no change in ionic strength, errors are not accumulated, and the measurement time is shorter than required for a sequential titration, minimizing problems like photodenaturation and/or photobleaching, then there is no difference in the magnitude of the fluorescence quench observed with or without  $Mg^{2+}$ .

There is another difference between our quench results and published reports. As the concentration of  $Mg^{2+}$  was increased in equilibrium titrations with  $K^+$ , the curves became sigmoidal, and it was concluded that  $K^+$  binds to multiple, interacting sites in the presence of  $Mg^{2+}$  (Hegyvary & Jorgensen, 1981). No change in shape of the amplitude versus  $[K^+]$  curves with or without  $Mg^{2+}$  was observed in the stopped-flow experiments (inset of Figure 2a). A plausible explanation of this difference is that the quench becomes extremely slow at high  $Mg^{2+}$  and low  $K^+$ ; for example, at 5 mM  $Mg^{2+}$  and 0.1 mM  $K^+$  the half-time of the quench reaction is approximately 30 s, so that the complete fluorescence change caused by an aliquot of titrant would not be observed in a sequential titration unless the experimenter waited more than a minute between additions.

**Role of  $Mg^{2+}$ .** If a reagent is directly involved in the mechanism of a reaction, either raising or lowering the potential energy barrier separating reactants from products, then both the forward and the reverse rate must be affected (principle of microscopic reversibility).  $Mg^{2+}$  affects only the reverse rate of the conformational change reported by fluorescein. Therefore, the transition state between  $E_1$  and  $E_2$  does not include the divalent cation.  $Mg^{2+}$  does not catalyze the conformational change. What is affected by  $Mg^{2+}$  is the affinity of the  $E_1$  enzyme conformation for  $K^+$ . Also affected by  $Mg^{2+}$  is the distribution of the enzyme with  $K^+$  bound between the two conformations at equilibrium. When  $K^+$  and  $Mg^{2+}$  are both bound, the  $E_2$  conformation of the Na,K-ATPase is much more stable than the  $E_1$  conformation. A simple explanation might be that the monovalent and divalent cations are farther apart in the  $E_2$  conformer. An increase in the spin-lattice relaxation time of  $^{205}Tl^+$  when  $P_i$  is added to a ternary complex of enzyme,  $Mn^{2+}$ , and  $Tl^+$  has been interpreted as an increase in the distance between  $Mn^{2+}$  and  $Tl^+$  from 4 to 5.4 Å when  $P_i$  is bound (Grisham et al., 1974). Vanadate acting as a transition-state analogue of  $P_i$  is thought to block the  $E_2 \rightarrow E_1$  transition (Karlsh et al., 1979).

Hegyvary and Jorgensen (1981) have suggested that  $Mg^{2+}$  binding and release may help to regulate the reaction cycle of Na,K-ATPase. Our results support their proposal, with the difference that formation of a ternary complex is sufficient to explain  $Mg^{2+}$  release and acceleration of the  $E_2 \rightarrow E_1$  transition without postulating a  $ME_2K$  conformation different enough to affect the quantum yield of bound fluorescein. The concentration of free  $Mg^{2+}$  in mammalian cells is thought to be buffered and in the range 0.2–1.0 mM (Flatman, 1991). Therefore,  $Mg^{2+}$  would dissociate from  $ME_2K$  formed in the forward half of the Albers–Post cycle by dephosphorylation, because  $K_{2KM} > 1$  mM. The upper pathway in eq 1 for reversal

of the conformational change ( $E_2K \rightarrow E_1K$ ) is still too slow to explain the *in vivo* pump rate, but  $Mg^{2+}$  release may also regulate nucleotide binding which dramatically increases the rate of the conformational change (Karlsh & Yates, 1978). ATP binds approximately an order of magnitude tighter to Na,K-ATPase in the presence of  $K^+$  alone than in the presence of both  $K^+$  and  $Mg^{2+}$  (Moczydlowski & Fortes, 1981). Since  $K_{1M} < 0.2$  mM,  $Mg^{2+}$  would rebind to the  $E_1$  conformer after  $K^+$  release and initiate the next cycle. A number of enzymes require  $Mg^{2+}$  concentrations approximating the free  $Mg^{2+}$  concentration in cells for activation, so that  $Mg^{2+}$  binding and release may be involved in the regulation of a variety of metabolic pathways.

## ACKNOWLEDGMENT

We wish to thank Shwu-Hwa Lin, Martin Stengelin, Vladimir Kasho, and Professors Robert A. Farley and Emil Reiser for participating in many valuable discussions of the work and for their careful proofreading of the manuscript. The hog kidneys from which sodium pump was isolated were kindly donated by Farmer John Clougherty Packing Company of Los Angeles.

## APPENDIX

A stopped-flow measurement can be thought of as a concentration-jump, chemical relaxation experiment in which the rise time of the step perturbation is  $t_d$ . The rate at which equilibrium is reestablished, or at which the system “relaxes”, is proportional to the magnitude of the disturbance

$$-\frac{d(\Delta[c])}{dt} = \frac{1}{\tau}(\Delta[c]) \quad (16)$$

where  $\Delta[c]$  is the difference between the instantaneous concentration of a reactant ( $[c]$ ) and its equilibrium value. The reciprocal of the constant of proportionality has units of time and is called the relaxation time ( $\tau$ ). For a step perturbation,

$$\Delta[c] = [c]_t - [c] \quad (17)$$

and the integrated form of eq 16 is

$$\Delta[c] = \Delta[c]_0 e^{-t/\tau} \quad (18)$$

$\Delta[c]_0$  is the difference between one-half the equilibrium concentration of reactant  $c$  before mixing ( $[c]_0$ ) and the equilibrium concentration of  $c$  after  $t_d$  ( $[c]_t$ ).

There are eight states, or differently liganded forms, of the two conformers in the model proposed for  $Mg^{2+}$  interaction with the Na,K-ATPase (Discussion; eq 1), so as many as seven relaxation times could be observed. All of the relaxation effects reported in this paper can be satisfactorily described by a single relaxation time. The presumed explanation is that the metal binding steps are too fast for resolution in a mixing experiment and are optically silent. The assumption that only the conformational transition between  $E_1$  and  $E_2$  causes a measurable difference in the quantum yield of bound fluorescein is justified *a posteriori* by the observation of only a single relaxation time. Therefore, quite generally, the rate at which the system reequilibrates is

$$-\frac{d[E_1]}{dt} = k_f[E_1K] + k_{mr}[ME_1K] - k_r[E_2K] - k_{mr}[ME_2K] \quad (19)$$

Lowercase  $k$  denotes a rate constant. The right-hand letter in the subscript means forward (f) or reverse (r), and an m

on the left stands for metalloenzyme. Rewriting eq 19 in terms of the fraction ( $\chi$ ) of each conformer in a particular liganded state, for example,

$$\chi_{E_1K} = [E_1K] / ([E_1]_{\text{free}} + [E_1M] + [E_1K] + [E_1Na] + [Me_1K] + [ME_1Na]) \quad (20)$$

gives

$$-\frac{d[E_1]}{dt} = k_f\chi_{E_1K}[E_1] + k_{mf}\chi_{ME_1K}[E_1] - k_r\chi_{E_2K}[E_2] - k_{mr}\chi_{ME_2K}[E_2] \quad (21)$$

Substituting expressions analogous to eq 17 for  $[E_1]$  and  $[E_2]$  gives

$$-\frac{d(\Delta[E_1])}{dt} = k_f\chi_{E_1K}[\bar{E}_1] - k_r\chi_{E_2K}[\bar{E}_2] + k_{mf}\chi_{ME_1K}[\bar{E}_1] - k_{mr}\chi_{ME_2K}[\bar{E}_2] + (k_f\chi_{E_1K} + k_{mf}\chi_{ME_1K})(\Delta[E_1]) - (k_r\chi_{E_2K} + k_{mr}\chi_{ME_2K})(\Delta[E_2]) \quad (22)$$

The first two terms in eq 22 cancel, because  $[\bar{E}_1]$  and  $[\bar{E}_2]$  are the equilibrium concentrations after mixing and therefore

$$k_f\chi_{E_1K}[\bar{E}_1] = k_r\chi_{E_2K}[\bar{E}_2] \quad (23)$$

Similarly, the third and fourth terms in eq 22 cancel. Finally, remembering that

$$\Delta[E_1] = -\Delta[E_2] \quad (24)$$

since the total enzyme concentration (denoted by subscript o)

$$[E]_o = [E_1] + [E_2] = ([E_1]_{\text{free}} + [ME_1] + [E_1K] + [E_1Na] + [Me_1K] + [ME_1Na]) + ([E_2K] + [ME_2K]) \quad (25)$$

is constant, gives

$$-\frac{d(\Delta[E_1])}{dt} = (k_f\chi_{E_1K} + k_{mf}\chi_{ME_1K} + k_r\chi_{E_2K} + k_{mr}\chi_{ME_2K})(\Delta[E_1]) \quad (26)$$

Comparing eq 26 with eq 16 confirms that  $1/\tau$  is given by eq 2 in the text. It is important to emphasize that no  $(\Delta[E_1])^2$  terms were discarded in the derivation of eq 26. Therefore, eq 2 in the text is valid for a large perturbation in the special case of a unimolecular reaction, like the protein conformational change reported by fluorescein. It is also important to note that, for the parallel pathways by which  $E_1$  is converted to  $E_2$  in the mechanistic scheme (eq 1), eq 26 predicts a single relaxation time.

The fractions of  $E_1$  and  $E_2$  in each of the reactive liganded forms can be expressed as functions of free ligand concentrations and equilibrium constants for the individual steps in eq 1 by substituting dissociation constants written in the form

$$K_{2KM} = \frac{[Mg^{2+}][E_2K]}{[ME_2K]} \quad (27)$$

into expressions like eq 20. The number in the subscript of  $K$  indicates the enzyme conformation. The letter on the right is the ligand that dissociates (M for  $Mg^{2+}$ , Na for  $Na^+$ , and K for  $K^+$ ), and there may be a letter in the middle if a ligand remains bound. In liganded forms of the enzyme, M is written on the left, and either Na or K, on the right, to indicate that  $Mg^{2+}$  binds to a different site than  $Na^+$  and  $K^+$ . Apparent constants for competitive binding of  $Na^+$  or  $K^+$  in the presence

of the other monovalent cation are indicated by writing (app) after the dissociation constant. For example,

$$K_{1K}(\text{app}) = K_{1K} \left( 1 + \frac{[Na^+]_o}{K_{1Na}} \right) \quad (28)$$

Since all of the individual reaction steps in eq 1 are coupled, any dissociation constant can be rewritten as the product of dissociation and association constants for reactions in an alternative, multistep pathway that results in the same net reaction. For example,

$$K_{1MK} = K_{1K} \frac{K_{1KM}}{K_{1M}} \quad (29)$$

In eqs 3–6, the free concentrations of  $Mg^{2+}$  and the monovalent cations are replaced by their total concentrations (e.g.,  $[Mg^{2+}]_o$ ), because the concentration of enzyme in the relaxation experiments was only about 1  $\mu M$ , so that the concentrations of the titrants were effectively buffered.

The amplitude of the  $K^+$  quench, expressed as relative change in fluorescence, is proportional to the fraction of the enzyme in the  $E_2$  conformation ( $\chi_2$ ) after equilibrium is reestablished.

$$\frac{\Delta F_o}{F}(\text{quench}) = \frac{[E_2]}{[E]_o} \frac{\Delta F_{\text{max}}}{F} = \chi_2 \frac{\Delta F_{\text{max}}}{F} \quad (30)$$

The amplitude of the  $Na^+$  reversal is calculated from the difference between the fraction of the enzyme in the  $E_1$  conformation ( $\chi_1$ ) before (0) and after ( $Na$ ) addition of  $Na^+$ .

$$\frac{\Delta F_o}{F}(\text{reversal}) = [\chi_1(Na) - \chi_1(0)] \frac{\Delta F_{\text{max}}}{F} \quad (31)$$

$\Delta F_{\text{max}}$  in eqs 30 and 31 is the extrapolated value at infinite titrant concentration. Since the enzyme may be distributed between the two conformations at the start of a mixing experiment, the theoretical maximum fluorescence change is the sum of the changes caused in separate experiments by saturating concentrations of  $K^+$  ( $E_2$  fluorescence level) and  $Na^+$  with no added  $K^+$  ( $E_1$  fluorescence level).  $\chi_1$  and  $\chi_2$  are found from their definitions (eqs 30 and 31) and the conservation equation (eq 25) by using equilibrium relationships like eq 27 to eliminate all concentration terms except the buffered cation concentrations and choosing one cation as the independent variable. Equation 8 in the Discussion is the resulting expression for the amplitude of quenches by  $K^+$  in the presence of  $Mg^{2+}$ , and eq 11 expresses the fraction of the enzyme in the  $E_1$  conformation for any choices of  $[K^+]$  and  $[Na^+]$  as a function of  $[Mg^{2+}]$ .

The final equations given in the text have been simplified by defining half-maximum concentrations and amplitude factors. Equation 9 reduces to

$$K_{0.5K} = \frac{K_{1K}}{K_c + 1} \quad (32)$$

when  $[Mg^{2+}] = 0$ , and eq 10 becomes

$$A_c = \frac{K_c}{K_c + 1} \quad (33)$$

with  $K_c = k_f/k_r$ .  $K_{0.5K}$  is the  $K^+$  concentration required for one-half the maximum fluorescence quench with apoenzyme, which is reduced by the factor  $A_c$ . The corresponding

relationships for metalloenzyme ( $[Mg^{2+}] = \infty$ ) are

$$K_{0.5MK} = \frac{K_{IMK}}{K_{mc} + 1} \quad (34)$$

and

$$A_{mc} = \frac{K_{mc}}{K_{mc} + 1} \quad (35)$$

with  $K_{mc} = k_{mf}/k_{mr}$ . Empirical half-maxima can also be defined for reversal reactions. However, there is no general functional form discernible for either the half-maximum or the amplitude factor, so the explicit equations fit to the data are given in the text (eqs 9, 10, 13, and 14). The notation adopted for half-maxima and amplitude factors is as follows: (1) The subscript 0.5 indicates that  $K$  corresponds to a half-maximum concentration. (2) The last letter in the subscript is the titrant. A final K denotes a quench experiment; a final M or a final Na, a reversal experiment. (3) Letters in parentheses denote other cations that were present but not necessarily bound.

## REFERENCES

- Carilli, C. T., Farley, R. A., Perlman, D. M., & Cantley, L. C. (1982) *J. Biol. Chem.* **257**, 5601-5606.
- De Pont, J. J. H. M., Helmich-de Jong, M. L., & Bonting, S. L. (1985) in *The Sodium Pump* (Glynn, I., & Ellory, C., Eds.) pp 733-738, The Company of Biologists Ltd., Cambridge, U. K.
- Faller, L. D., & Johnson, A. M. (1974a) *Proc. Natl. Acad. Sci. U.S.A.* **71**, 1083-1087.
- Faller, L. D., & Johnson, A. M. (1974b) *FEBS Lett.* **44**, 298-301.
- Faller, L. D., Diaz, R. A., Scheiner-Bobis, G., & Farley, R. A. (1990) *FASEB J.* **4**, A1962.
- Faller, L. D., Diaz, R. A., Scheiner-Bobis, G., & Farley, R. A. (1991a) *Biochemistry* **30**, 3503-3510.
- Faller, L. D., Scheiner-Bobis, G., & Farley, R. A. (1991b) in *The Sodium Pump: Recent Developments* (Kaplan, J. H., & De Weer, P., Eds.) pp 357-361, The Rockefeller University Press, New York.
- Flatman, P. W. (1991) *Annu. Rev. Physiol.* **53**, 259-271.
- Frost, A. A., & Pearson, R. G. (1953) *Kinetics and Mechanism*, pp 74-99, Wiley, New York.
- Garay, R. P., & Garrahan, P. J. (1973) *J. Physiol.* **231**, 297-325.
- Glynn, I. M. (1985) *Enzymes Biol. Membr.* **3**, 62-65.
- Grell, E., Warmuth, R., Lewitzki, E., & Ruf, H. (1991) in *The Sodium Pump: Recent Developments* (Kaplan, J. H., & De Weer, P., Eds.) pp 441-445, The Rockefeller University Press, New York.
- Grell, E., Warmuth, R., Lewitzki, E., & Ruf, H. (1992) *Acta Physiol. Scand.* **146**, 213-221.
- Grisham, C. M., & Mildvan, A. S. (1974) *J. Biol. Chem.* **249**, 3187-3197.
- Grisham, C. M., & Mildvan, A. S. (1975) *J. Supramol. Struct.* **3**, 304-313.
- Grisham, C. M., & Hutton, W. C. (1978) *Biochem. Biophys. Res. Commun.* **81**, 1406-1411.
- Grisham, C. M., Gupta, R. K., Barnett, R. E., & Mildvan, A. S. (1974) *J. Biol. Chem.* **249**, 6738-6744.
- Hegyvary, C., & Jorgensen, P. L. (1981) *J. Biol. Chem.* **256**, 6296-6303.
- Henkens, R. W., Watt, G. D., & Sturtevant, J. M. (1968) *Biochemistry* **7**, 1874-1878.
- Jorgensen, P. L. (1974) *Biochim. Biophys. Acta* **356**, 36-52.
- Karlish, S. J. D. (1980) *J. Bioenerg. Biomembr.* **12**, 111-135.
- Karlish, S. J. D., & Yates, D. W. (1978) *Biochim. Biophys. Acta* **527**, 115-130.
- Karlish, S. J. D., Beaugé, L. A., & Glynn, I. M. (1979) *Nature* **282**, 333-335.
- Kuriki, Y., Halsey, J., Biltonen, R., & Racker, E. (1976) *Biochemistry* **15**, 4956-4961.
- Matheson, I. B. C. (1987) *Anal. Instrum.* **16**, 345-373.
- Moczydlowski, E. G., & Fortes, P. A. G. (1981) *J. Biol. Chem.* **256**, 2346-2356.
- O'Conner, S. E., & Grisham, C. M. (1980) *FEBS Lett.* **118**, 303-307.
- Post, R. L., Hegyvary, C., & Kume, S. (1972) *J. Biol. Chem.* **247**, 6530-6540.
- Rendi, R., & Uhr, M. L. (1964) *Biochim. Biophys. Acta* **89**, 520-531.
- Robinson, J. D. (1975) *Biochim. Biophys. Acta* **384**, 250-264.
- Robinson, J. D. (1989) *Biochim. Biophys. Acta* **997**, 41-48.
- Robinson, J. D., Hall, E. S., & Dunham, P. B. (1977) *Nature* **269**, 165-167.
- Skou, J. C., & Esmann, M. (1983) *Biochim. Biophys. Acta* **727**, 101-107.
- Stewart, J. M. MacD., & Grisham, C. M. (1988) *Biochemistry* **27**, 4840-4848.
- Wadsö, I. (1962) *Acta Chem. Scand.* **16**, 479-486.
- Wold, F. (1971) *Enzymes* **4**, 517.